

Conductance quantization in Si/SiGe wires

G. Scappucci,^{1,*} L. Di Gaspare,¹ E. Giovine², A. Notargiocomo,² R. Leoni² and F. Evangelisti^{1,2}

¹*Dipartimento di Fisica "E. Amaldi", Università Roma TRE, V. Vasca Navale 84, 00146 Roma, Italy*

²*Istituto di Fotonica e Nanotecnologie, IFN-CNR, Via Cineto Romano 42, 00156 Roma, Italy*

PACS numbers: 73.63.Nm

Abstract

Intriguing conductance quantization in units of approximately $1e^2/h$ is observed in strongly confined quantum point contacts fabricated by etching Si/SiGe heterostructure wires in bent geometries. Non-linear conductance measurements performed depleting the wires at fixed mode-energy separation show evidences of the formation of a half $1e^2/h$ plateau, supporting the speculation that adiabatic transmission occurs through 1D modes with complete removal of valley and spin degeneracies.

It is generally accepted that the conductance of one-dimensional ballistic wires is quantized in units $G_0=2e^2/h$ (here e is the electron charge and h the Planck's constant) when an adiabatic transmission via spin-degenerate modes is taking place [1,2]. However, deviations from the regular $N G_0$ values (N is the number of the occupied one-dimensional (1D) modes) have appeared in the literature. In particular, an additional plateau at 0.5-0.7 G_0 , usually referred to as "0.7 structure" and originally evidenced by Thomas et al. [3], has received a great deal of attention recently [4-9]. Its presence is assumed to signal the occurrence of non negligible correlation effects, although it does not seem that a general consensus on its origin has been reached as yet [10-15].

The large majority of 1D conductance investigations have been performed on systems based on GaAs heterostructures. Few works have dealt with the 1D ballistic transport in silicon or Si/SiGe heterostructures. In these systems, due to the presence of valley degeneracy for the electrons, it is expected that the conductance would be quantized in multiple integers of $4e^2/h$. Indeed, conductance quantization in units $4e^2/h$ was reported in split-gate quantum point contacts in Si inversion layers [16] and in a SiGe 2DEG [17], as well as in etched constrictions in SiGe 2DEG [18]. Quite to the contrary, well defined and wide plateaus at multiples of $2e^2/h$ were found in vertical silicon structures [19].

We report here the presence of a conductance plateau at $\sim 0.5 G_0$, akin to the "0.7 structure", and evidence for a quantization in unit e^2/h in Si/SiGe heterostructure quantum point contacts obtained by etching away the side material.

The devices were fabricated on two samples (A and B) containing a high mobility two-dimensional electron gas located 70 nm below the surface of Si/SiGe modulation doped heterostructures grown by chemical vapor deposition. Details of the layer sequence thickness as well as the structural and morphological properties of the SiGe 2DEG's samples are described elsewhere [20]. A standard analysis of the low-field magnetoresistance at $T=300\text{mK}$ of mesa-etched Hall bars gives an estimate of

the 2DEG carrier density $9.8 \times 10^{11} \text{ cm}^{-2}$ and $n_{2D} = 7.62 \times 10^{11} \text{ cm}^{-2}$, electronic mobility $\mu = 4.1 \times 10^4 \text{ cm}^2/\text{Vs}$ and $6.7 \times 10^4 \text{ cm}^2/\text{Vs}$ for samples A and B, respectively.

The devices were obtained by shaping the 2DEG in a bent nanowire geometry fabricated by electron-beam lithography (EBL) and reactive ion etching (see insets of Fig. 1). The nanowires were defined in the inner region of 2DEG mesa structures designed so as to allow an electrical characterization of the device both in a two- and four-terminal configuration. Geometrical constrictions that act as quantum point contacts (QPC) were introduced in a controlled manner by the lateral displacement of a segment of the wires. With this approach, on the same 2DEG sample, nanostructures with constrictions of decreasing geometrical width were obtained by increasing the lateral shift of the nanowire segment. Two different types of devices were prepared, with a single (sample A) and with two constrictions (sample B). As the constrictions become narrow and their width comparable with the Fermi wavelength, that in our 2DEG is estimated to be $\lambda_F \sim 50 \text{ nm}$, they act as quantum points contacts connecting the source and drain.

The devices were completed by defining a central metallic control gate by EBL and lift-off. Devices with a single constriction had a Ti/Au Schottky-barrier gate, while a MOS structure was used for the gates of two-constriction devices. Transport measurements were performed both in a two- and four-terminals configuration in a ^3He refrigerator in the 300mK - 4.2K temperature range using standard ac lock-in techniques with a small source-drain excitation at a frequency of 17 Hz.

Etched wires have strong lateral confining potentials. Furthermore, due to sidewall depletion caused by the surface states generated by the fabrication process, the constrictions have an effective width much smaller than the lithographic one [21]. Also, these states completely screen the electric field imposed by the gate on the lateral walls [22]. As a consequence, the gate varies the carrier concentration without affecting the width of the quantum point contact. Therefore, in our devices we can follow the effect of depleting the wire at fixed mode-energy separation.

The linear-response conductance (i.e. $G=dI/dV_{SD}$ around $V_{SD} \sim 0$) versus the gate voltage V_G is reported in Fig. 1 for the three devices shown in the insets. While the curve in panel (a) is a two-terminal differential conductance, corrected for a series resistance $R_S = 19.4 \text{ k}\Omega$, originating from both the 2DEG leads and the source and drain contacts, the curves in panel (b) are four-terminal differential conductances, where no corrections have been made. All the curves were highly reproducible upon cycling V_G from positive to negative voltages or the temperature from 0.350K to 4.2K or to room temperature.

Curve (a) exhibit plateau-like structures close to multiple integers of $0.5 G_0$. It is worthy of notice that in no case we would be able to subtract a R_S such as to recover plateaus spaced by $1 G_0$ or $2 G_0$. A similar behavior of the plateau-like features is found in the left curve of panel (b), although the first and third plateaus are slightly below $0.5 G_0$ and $1.5 G_0$, respectively. In this curve an extra structure is also present at $G \sim 0.1 G_0$. In the right curve of panel (b) plateaus are present at $0.5 G_0$ and $1.5 G_0$, while the $1 G_0$ structure has acquired a peak-like character and two peaks are present for G below $0.5 G_0$. We interpret the peak-like structures below $0.5 G_0$ as due to resonant states that form in the double-bend geometry, which acts as a cavity for the electrons [23]. Notice that in the case of device in panel (a) we could follow a reduction of conductance of three orders of magnitude after pinch-off without finding any resonant-like peak. The peak-like character of the $1 G_0$ plateau is also attributed to the presence of a resonance [24]. These resonances will be analyzed in a forthcoming paper. In the following we will discuss the half integer quantization, which was, to our knowledge, not previously reported in Si/Ge heterostructures.

Significant information on the $\sim 0.5 G_0$ (i.e. $\sim e^2/h$) plateau have been obtained from the non-linear transport measurements, i.e. the curves of the differential conductance G as a function of finite dc source-drain bias V_{SD} for different gate voltages V_G . In Fig. 2(a) we report a series of G - V_{SD} curves

relative to the device with the single constriction, measured in sequence, progressively decreasing the gate voltage from -0.4 to -0.2 V in steps of 2.5 mV. This gate bias range covers the region where the linear conductance reported in Fig. 1(a) develops the $\sim 0.5 G_0$ feature. As a preliminary analysis, we point out that for $|V_{SD}| > 10$ mV the conductance value of all the $G-V_{SD}$ curves, irrespectively to the gate voltage bias, start to decrease tending toward zero, a clear indication of current saturation. The likely origin of this saturation will be discussed later on. In the $|V_{SD}| < 10$ mV bias range we observe clear asymmetries in the curves, even around zero V_{SD} , that we address in terms of a self-gating effect [5]. We correct our data for this electrostatic effect as in Ref. [5] considering only the symmetric combination $G^*(V_{SD}) = \frac{1}{2}[G(+V_{SD})+G(-V_{SD})]$ of the $G(V_{SD})$ traces. We report the corrected $G^*(V_{SD})$ curves in Fig. 2(b).

The curves in Fig. 2(b) show an overall evolution very similar to that found in both GaAs quantum point contacts [25] for the $2e^2/h$ quantization and carbon nanotubes for the e^2/h quantization [26]. This evolution can be accounted for by using the single mode contribution of the Landauer theory for each of the plateau seen in Fig. 1. We see in Fig. 2(b) that for large negative values of V_G the conductance is negligible at small V_{SD} , meaning that both electrochemical potentials μ_L (left contact) and μ_R (right contact) are below the onset energy E_0 of the first 1D band. As the negative gate voltage is decreased to -0.34V [arrow (1)], the electrochemical potential at $V_{SD}=0$ V (i.e. $\mu=\mu_L=\mu_R$) is aligned to the edge of the first 1D band E_0 , as confirmed by the clear observation of the change of curvature of the neighboring $G(V_{SD})$ curves. A further decrease of the negative gate bias brings about a rapid increase of the linear conductance (G at $V_{SD} \sim 0$) toward the value $\sim 0.5 G_0$, corresponding to μ entering progressively into the E_0 band. At $V_{SD} \sim 4$ mV different traces merge at a value close to $0.25 G_0$ indicating the formation of the half e^2/h plateau, as expected for E_0 lying between μ_L and μ_R [27]. Around $V_G \sim -0.3125$ V, that corresponds to the $0.5 G_0$ plateau in the $G-V_G$ curve of Fig 1(a), several curves bundle at $0.5 G_0$ [arrow

(2)]. An interval of V_G values then follows, where the range of conductance equal to $0.5 G_0$ progressively spreads to higher values of V_{SD} , but no contributions to the conductance come from the next mode. Finally, for further reduction of negative V_G , the next mode starts to contribute, first for large values of V_{SD} , then to the linear conductance. We see indications of the formation of a $\sim 0.75 G_0$ plateau at $V_{SD} \sim 4$ mV and $V_G = -0.215$ V [arrow (3)].

Finally, we comment on the drastic decrease of conductance for $V_{SD} >\sim 10$ mV. For sufficiently large source-drain bias the bottom of the electron band of the high-energy contact will become higher than the mode onset and, eventually, the electrochemical potential of the low-energy contact will drop below the bottom of the electron band of the high-energy contact. In these conditions the current saturates at a value independent of bias voltage and the differential conductance drops to zero. Another possible effect causing a current saturation is the electron drift-velocity saturation due to carrier heating at large bias and the onset of non-ballistic transport [18].

In Fig. 2(c) we report the curves of the conductance G versus V_G as measured, in a successive cool-down, at different V_{SD} dc bias that confirm the evolution we have described. The curves at $V_{SD} = 0$ and 8mV provide a clear evidence of the presence in the linear conductance of $0.5 G_0$ and $1 G_0$ steps evolving at large V_{SD} to $0.25 G_0$ and $0.75 G_0$ structures, respectively. In the curve at $V_{SD} = +24$ mV no significant structures appear due to current saturation.

We estimate the energy spacing $\Delta E_{1,0}$ between the first two 1D subbands by analyzing the non-linear conductance curves at fixed gate voltage with the Zagoskin method [28]. In a symmetric QPC, when μ lies between the edges of two successive subbands, the subband energy spacing is $\Delta E = e/2(V_1+V_2)$. Here V_1 and V_2 are the source-drain voltages at which the first two extrema occur in the derivative dG/dV_{SD} , i.e. the position of the inflections of the $G(V_{SD})$ curves at fixed V_G . Depending on the position of μ below or above the midway between the edges of successive 1D subbands, V_1 is a

minimum and V_2 is a maximum or vice versa. In Fig. 3 we report two representative dG/dV_{SD} curves obtained by numerical differentiation of the curves at $V_g = -0.3325$ V and $V_g = -0.2925$ V of Fig. 2(b). As depicted schematically in the insets, at these gate voltages the electrochemical potential μ lies below and above, respectively, the midway between the first two 1D subbands. Consistently with the relative position of the chemical potential and the band edges suggested, we found that V_1 is a minimum and V_2 a maximum for the curve at $V_g = -0.3325$ V. The vice versa occurs for the curve at $V_g = -0.2925$ V. The subband spacing, calculated according to $\Delta E = e/2(V_1 + V_2)$, is $\Delta E_{1,0} \sim 4.4$ meV for both curves. This analysis was repeated for other curves, at different gate bias, in which we could mark unambiguously the position of well-resolved extrema. We found that the subband spacings does not vary significantly with the gate voltage. This confirms that, in our quantum point contact, changes in the gate voltage result in a variation of the carrier concentration without altering significantly its width.

It is worth emphasizing that, although the overall behavior of the linear and non-linear conductance upon changing the gate bias can be explained by the single mode contributions of the Landauer theory, a removal of all degeneracies and a quantization in units e^2/h is required to account for the data. The removal of the valley degeneracy is likely to be the result of the strong confining potential, which might split the odd and even states formed by combining the k and $-k$ states at the two minima [29]. Indeed, unambiguous removal of the valley degeneracy was also present in the conductance curves reported in Ref. [19] on etched vertical wires.

More intriguing is the presence of the $0.5 G_0$ plateau. Although the features are not as well resolved as in the GaAs case due to the much shorter mean free path of electrons in the SiGe heterostructures, the overall similarity between the present data and those of the “0.7 structure” is undeniable and we conclude that we have observed a similar effect in the Si/SiGe system.

The “0.7 structure” was originally related to correlation effects involving the electron spin [3]. Since then a great deal of efforts has been dedicated to the understanding of its microscopic origin. One

model attributes the effect to a spontaneous spin polarization in the QPC due to exchange interaction [11,12]. Another model [13] claims the formation of a dynamical local moment in the QPC resulting in a spin splitting due to the local Coulomb interaction energy U . This model would account for the observation of many features of Kondo physics in QPC [7]. Other models suggest electron-phonon coupling [14] or Wigner crystallization [10] as source of the effect. The observation we report of an analogous phenomenon in a completely different system like the Si/Ge QPC is relevant to the problem, since a possible theoretical model is required to be valid also for the material parameters of the Si 2DEG.

Previous investigations on the conductance of Si/Ge QPC did not find the half G_0 quantization. We speculate that a strong confining potential is required in order to have the degeneracy removal and that the techniques adopted in Ref. [16-18] did not provide it. A strong confining potential is present in Ref. [19] and there the conductance curves do show a structure at 0.5-0.7 G_0 , although the authors do not mention it. We are currently investigating the relationship between potential strength and shape and the presence of the half G_0 quantization.

This work was partially supported by the FIRB project RBNE01FSWY “Nanoelettronica” and the FISR project “Nanotecnologie per dispositivi di memoria ad altissima densità”.

References

* Present address: School of Physics, University of New South Wales, Sydney NSW 2052, Australia.

- [1] B. J. van Wees *et al.* Phys. Rev. Lett. **60**, 848 (1988).
- [2] D. A. Wharam *et al.*, J. Phys. C **21**, L209 (1988).
- [3] K. J. Thomas *et al.*, Phys. Rev. Lett. **77**, 135 (1996); K. J. Thomas *et al.*, Phys. Rev. B **58**, 4846 (1998); K. J. Thomas *et al.*, Phys. Rev. B **61**, R13365 (2000).
- [4] P. Ramvall, N. Carlsson, I. Maximov *et al.*, Appl. Phys. Lett. **71**, 918 (1997).
- [5] A. Kristensen *et al.*, Phys. Rev. B **62**, 10950 (2000).
- [6] D. J. Reilly *et al.*, Phys. Rev. B **63**, 121311(R) (2001); D. J. Reilly *et al.*, Phys. Rev. Lett. **89**, 246801 (2002).
- [7] S. M. Cronenwett, H. J. Lynch, D. Goldhaber-Gordon *et al.*, Phys. Rev. Lett. **88**, 226805 (2002).
- [8] R. dePicciotto, L. N. Pfeiffer, K.W. Baldwin, and K.W. West, Phys. Rev. Lett. **92**, 036805 (2004); R. dePicciotto, L. N. Pfeiffer, K.W. Baldwin, and K.W. West, Phys. Rev. B **72**, 033319 (2005).
- [9] R.W. Giannetta *et al.*, Physica E **27**, 270 (2005).
- [10] B. Spivak and F. Zhou, Phys. Rev. B **61**, 16730 (2000).
- [11] H. Bruus *et al.*, Physica E **10** 97 (2001).
- [12] K. F. Berggren and I. I. Yakimenko, Phys. Rev. B **66**, 085323 (2002); A. A. Starikov, I. I. Yakimenko, and K. F. Berggren, Phys. Rev. B **67**, 235319 (2003).
- [13] Y. Meir, K. Hirose, N.S. Wingreen, Phys. Rev. Lett. **89**, 196802 (2002); K. Hirose, Y. Meir, and N.S. Wingreen , Phys. Rev. Lett. **90**, 026804 (2003).
- [14] G. Seelig and K. A. Matveev, Phys. Rev. Lett. **90**, 176804 (2003).
- [15] O. P. Sushkov, Phys. Rev. B **67**, 195318 (2003).
- [16] S. L. Wang, P.C. vanSon, B.J. vanWees, and T.M. Klapwijk, Phys. Rev. B **46**, R12873 (1992).

[17] D. Tobben, D. A. Wharam, G. Abstreiter, J. P. Kolthaus, and F. Schaffler, *Semicond. Sci. Technol.* **10**, 711 (1995).

[18] U. Wieser, U. Kunze, K. Ismail, and J. O. Chu, *Appl. Phys. Lett.* **81**, 1726 (2002).

[19] K. Nishiguchi and S. Oda, *Appl. Phys. Lett.* **76**, 2922 (2000).

[20] L. Di Gaspare *et al.*, *Appl. Phys. Lett.* **79**, 2031 (2001); L. Di Gaspare *et al.*, *Mater. Sci. Eng. B* **89**, 346 (2002).

[21] E. Giovine *et al.*, *Nanotechnology* **12**, 132 (2001).

[22] G. Curatola and G. Iannaccone, *J. Appl. Phys.* **95**, 1251 (2004).

[23] G. Scappucci *et al.*, *Phys. Rev. B* **71**, 245311 (2005).

[24] J. Bardarson *et al.*, *Phys. Rev. B* **70**, 245308 (2004).

[25] N. K. Patel *et al.*, *Phys. Rev. B* **44**, 13549 (1991).

[26] M. J. Biercuk, N. Mason, J. Martin, A. Yacoby, and C. M. Marcus, *Phys. Rev. Lett.* **94**, 026801 (2005).

[27] L. P. Kouwenhoven *et al.*, *Phys. Rev. B* **39**, R8040 (1989).

[28] A. M. Zagoskin, *JETP Lett.* **52**, 435 (1990).

[29] A. B. Fowler, F. F. Fang, W. E. Howard, and P. J. Stiles, *Phys. Rev. Lett.* **16**, 901 (1966); T. Ando, A. B. Fowler, and F. Stern *et al.*, *Rev. Mod. Phys.* **54**, 437 (1982).

FIGURE CAPTIONS

FIG.1.(a) Differential conductance G versus gate voltage V_G for the device shown in the inset in units of the conductance quantum $G_0=2e^2/h$. Measurement temperature was 450 mK; (b) Same as (a) for two devices shaped as in the inset. Measurement temperatures were 450 mK – left, 300 mK- right.

FIG. 2. (a) Plot of the non-linear differential conductance G versus source-drain voltage V_{SD} for different values of gate bias V_G measured at $T=450\text{mK}$. Both G and V_{SD} are corrected by subtracting a $19.4\text{ k}\Omega$ series resistance. Conductance roll-off at $V_{SD}>\sim 10\text{mV}$ is caused by current saturation. In (b) the symmetrized plot corrected for self-gating effect is reported. Arrows highlight the gate bias values at which significant evolution of the curves is observed, due to the relative alignment between the electrochemical potential μ and the 1D band edges. (c) Differential conductance G versus V_G for three values of V_{SD} bias. The formation of semi-plateau at finite source-drain bias is highlighted by the lowering of the $\sim 1G_0$ and $\sim 0.5G_0$ structures to $\sim 0.75G_0$ and $\sim 0.25G_0$ respectively. Traces are offset horizontally. Arrows are a guide for the eyes.

FIG. 3. Conductance derivative dG/dV versus source-drain bias V_{SD} at different gate bias at $T=450\text{ mK}$. The curves are offset vertically. Insets depict the position of the electrochemical potentials μ_L and μ_R with respect to the first two 1D subbands. Open circles in each curve mark V_1 and V_2 , respectively.

Figure 1

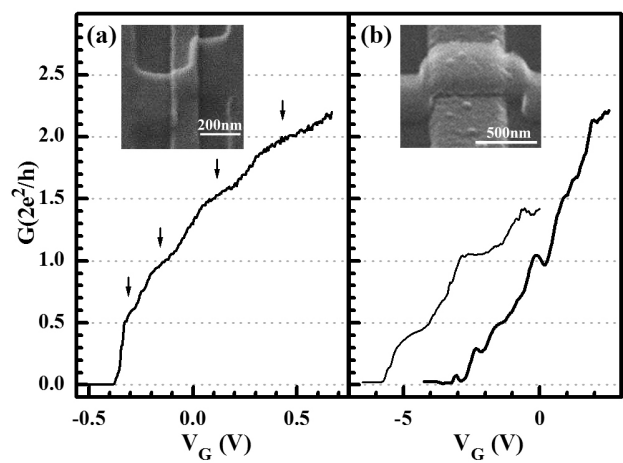


Figure 2

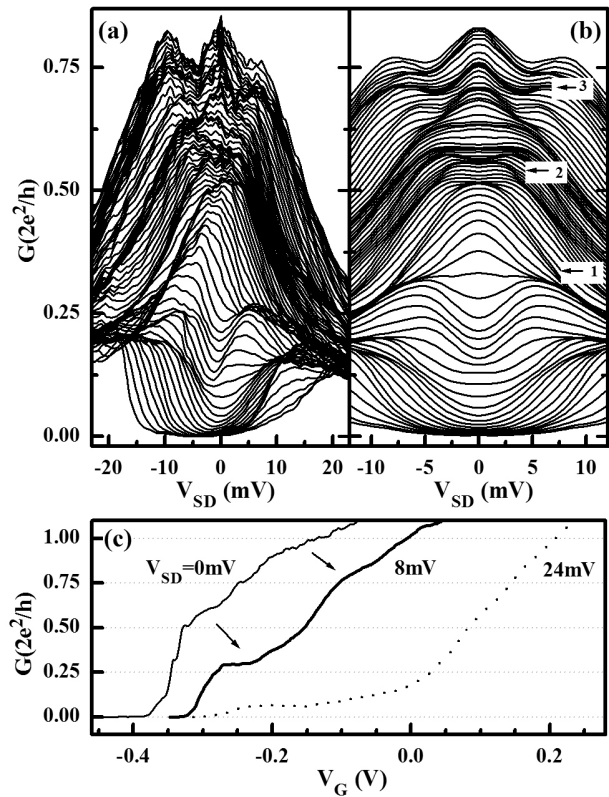


Figure 3

